Chapter 6

Calibration of the Devices

6.1 Introduction

This chapter describes the two distinct procedures used to calibrate the instruments developed in Part II.

The first one is dedicated to the camera calibration, and is performed by means of a Matlab® toolbox, presented in Section 6.2.

The second one, inspired from [29], concerns the laser plane calibration.

6.2 Camera Calibration

6.2.1 In Practice

As announced in the introduction, the camera calibration is performed by a Matlab® toolbox developed by Jean-Yves Bouguet at the California Institute of Technology [30]. See also [31].

The interested reader will find in Appendix A the mathematical details behind this algorithm, inspired from [11].

Note that this calibration operation is distinct from the laser plane calibration (see Section 6.3), and thus independent from the considered structured lighting application.

The procedure is as follows:

a) Print a pattern and attach it to a planar surface. We used a checker pattern represented on Fig. 6.1. Note that the geometry of the pattern (i.e. the size of the squares) may be unknown, since we are using a *photogrammetric* technique, where the feature points detected on the pattern are re-estimated at each iteration stage of the calibration;

b) Take a few images (at least three) of this model plane under different orientations, by moving either the plane or the camera. See Fig. 6.2 for an example of image;

c) Click on the four corners of the checker pattern. The Matlab® toolbox then automatically detects the feature points in the images, i.e. the corners of each checker square. Fig. 6.3 shows these points;

d) Estimate the five first intrinsic parameters;

e) Estimate the two coefficients of the radial distortion;

f) Iteratively refine all the parameters.

The last three steps are fully carried out by the Matlab® toolbox.

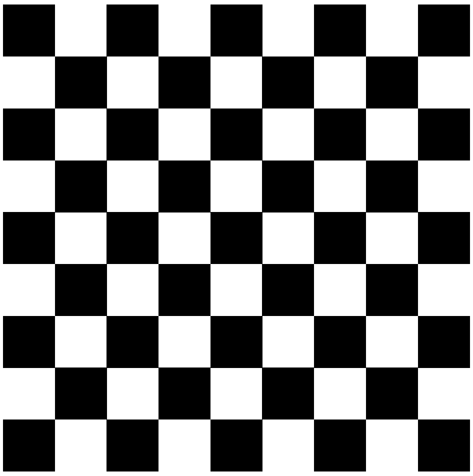

Fig. 6.1. Checker pattern used as model plane.

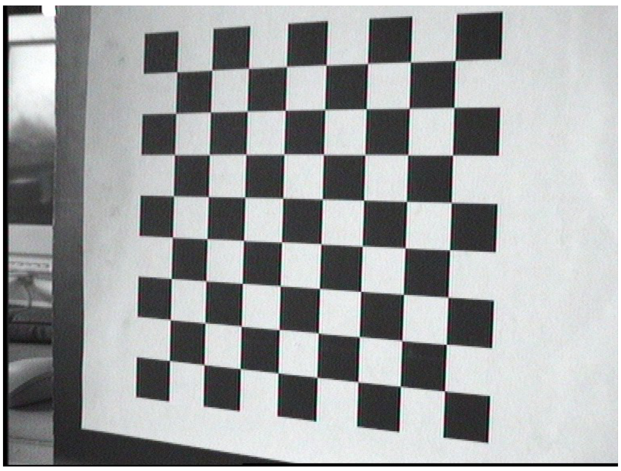

Fig. 6.2. Checker pattern. Camera capture.

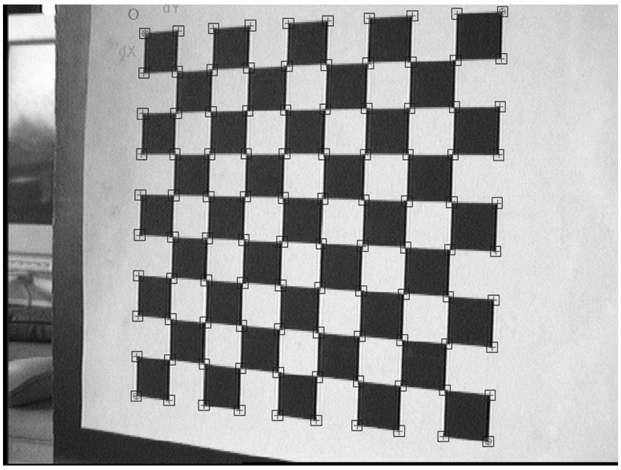

Fig. 6.3. Checker pattern. Feature points detected.

6.2.2 Performances

Calibration

In order to evaluate the repeatability of the camera calibration procedure, we acquired 50 images of the checker pattern under various orientations, and performed 50 different calibrations, each time using 10 randomly chosen images amongst the whole set. The mean values of the camera parameters, together with the standard deviations, are summarized on TABLE 6.1. Fig. 6.4 illustrates the results for the two parameters f_y and $X_{pix,0}$ (the figures are similar for the other ones).

These figures allow us to make the following observations:

- $f_x \cong f_y$, meaning that the pixels are indeed approximatively square;
- knowing that one pixel is 1/160-mm wide, we obtain $f \cong 8$ mm, which is coherent with the characteristics of the lens (Lens #1 in Section 4.2.2);
- $X_{pix,0}$ and $Y_{pix,0}$ have plausible values, i.e. corresponding more or less to the center of the CCD sensor, composed of 768x576 pixels (Camera #1 in Section 4.2.1);
- the standard deviation on these first four parameters is of the order of 0.1%, which is really excellent. See Section 7.4 to see the impact of these results on the accuracy of laser triangulation under structured lighting itself;

- γ is so low that it is pertinent to neglect it;
- there is only a small amount of distortion introduced by the lens (which explains the rather bad results regarding the standard deviations of k_1 and k_2). We will see in Part II that the introduction of an interference filter in front of the CCD sensor raises the distortion level.

TABLE 6.1. Values and Dispersions of the Camera Parameters

parameter	mean value	standard deviation
f_x	1218.6 pixels	0.12%
f_y	1238.8 pixels	0.12%
$X_{pix,0}$	394.6 pixels	0.14%
$Y_{pix,0}$	278.5 pixels	0.18%
γ	$-1.2\ 10^{-4}$ pixels	13%
k_1	0.2	31%
k_2	0.28	21%

Correction of the distortion

To appreciate the quality of the correction of the distortion, we selected—randomly—one of the 50 images mentioned hereabove, and studied how a set of feature points of the calibration pattern (i.e. the corners of the squares) in the same row, are transformed. On Fig. 6.5, the empty circles materialize the initial positions of the feature points, and the gray squares the same points after the correction of the distortion. One clearly sees the improvement (they describe a parabolic curve before the correction, and an almost perfect straight line after). The standard deviation of the corrected points regarding a perfectly straight line confirms the quality of the procedure: it is of 0.15 pixels. One also sees that the difference in position of the feature points before and after the correction of the distortion can go up to 1 pixel (despite the rather low level of distortion of the lens), which is nonnegligible (See Chapter 7, where one analyzes the influence of location errors).

6.3 Laser Plane Calibration

6.3.1 Positioning of the Problem

Instrumentation relying on laser triangulation under structured lighting is relevant only if the geometrical parameters of the instruments—presented in Chap-

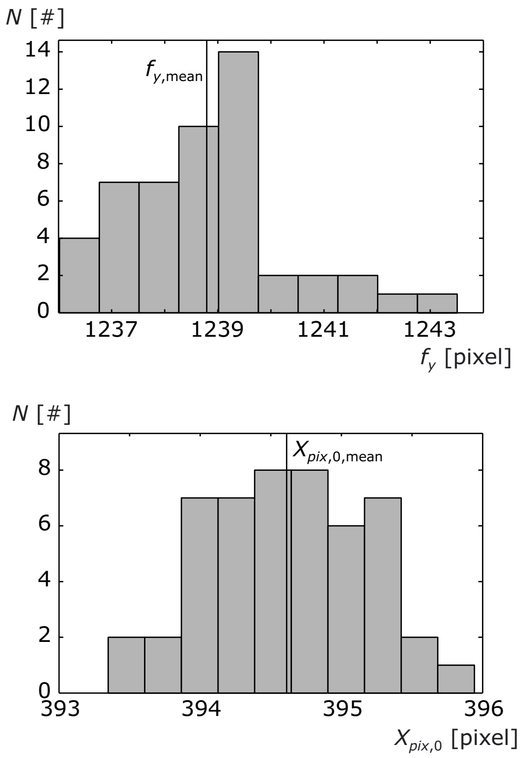

Fig. 6.4. Repeatability of the camera calibration, for f_x and $X_{pix,0}$.

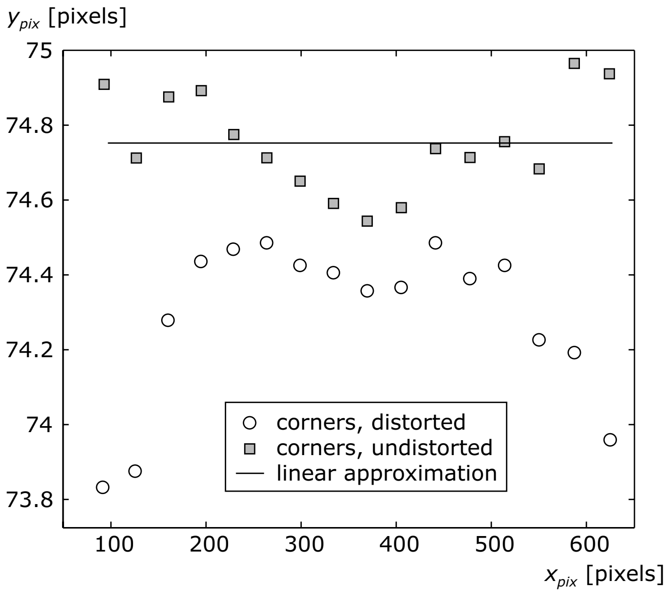

Fig. 6.5. Correction of the distortion: evaluation of the performances.

ters 2 and 3—are known with a high accuracy. By means of the technique presented in Section 6.2, we can consider the camera parameters as accurately determined. As for those concerning the laser plane(s), they still remain to be calibrated.

Let Q be the dimensional quantity measured by the instrument to calibrate. Generally speaking, this quantity can be written as a function of the camera and laser plane parameters U_c and U_l respectively, and of the position P_{pix} of one or several laser points in the image plane:

$$Q = Q\left(U_c, U_l, P_{pix}\right) \tag{6.1}$$

Depending on the application (quality of the camera lens, amount of laser planes needed, number of points to identify on the image), the dimensions of U_c, U_l and P_{pix} will vary, but at this point we would like to stay as general as possible.

Let ρ_Q be the relative error on Q:

$$\rho_Q = \frac{Q - Q_r}{Q_r} \tag{6.2}$$

where Q_r is the real value of the measured quantity Q. This error has of course to be the smallest as possible for the considered application.

Consequently, one can say that calibration is the optimization process consisting in finding the laser parameters U_l minimizing the relative error ρ_Q for a set of N measurements made on known objects (U_c is known and P_{pix} is measured on the image).

Note that technically speaking, ρ_Q is a multivariate differentiable function, the parameters of which are unconstrained (i.e. the laser parameters are independent from each other).

A various amount of methods can be used to solve this minimization problem [29]. The most popular is probably gradient descent, that we actually used. It is described hereafter.

6.3.2 Gradient Descent

The *gradient descent method*, or *steepest-descent method*, is an iterative optimization technique used for the unconstrained minimization of multivariate differentiable functions.

It leads to an estimate of the laser parameters U_l that minimizes the mean relative error ρ_Q on the N measurements performed on known objects.

The partial derivatives of the error in relation to the parameter vector U_l are used with an adequate weight function β—its value is empirically chosen to assure a fast but smooth convergence—to correct U_l:

$$U_{l,i,j+1} = U_{l,i,j} - \beta \left(\frac{\partial \rho_Q}{\partial U_l} \right)_{i,j} \rho_{Q,i,j} \tag{6.3}$$

where i is the measurement number ($i = 1 \dots N$) and j the iteration number. After each iteration, the parameter vector U_l is replaced by the mean value of the N vectors provided by (6.3), and the procedure is stopped when the change of U_l between two successive iterations is negligible ($< 0.01\%$) with regard to the experienced final accuracy, or when a maximum number of iterations has been performed.

This method requires an initial estimation $U_{l,0}$ of the parameter vector, e.g. estimated by dimensional measurements on the instrument. Note that a bad starting value of U_l can lead to a local minimum of the relative error: intuitively, observing (3.7), we see that erroneous combinations of the laser plane parameters can somehow produce "not too bad" results. It is thus important to choose their initial value with care.

Depending on the case, it takes from 100 to 2000 iterations to find the correct estimate of the parameters.

The main advantage of this method is that it can be easily implemented in the C++ environment, which was exclusively used in this thesis. Beside that, the calculation of the partial derivative and the choice of β can be tedious.

6.3.3 In practice

The purpose of this section is to show how the laser plane calibration is done in practice. This procedure being application-dependent, at this point we have to anticipate the developments of Part II, presenting our own devices. We chose to illustrate the calibration with the diameter measurement of cylindrical objects, detailed in Chapter 9.

The aim being only to be illustrative, we restrict ourselves to the case of a cylinder whose axis is transversal to the camera plane (discussed in Sections 9.2 and 9.4), even though the general case of a randomly tilted cylinder will also be studied (Sections 9.7–9.10). In this simple case, one laser plane is sufficient, and the expression of the cylinder radius is [see (9.4)]:

$$R = \frac{Y_1\,(X_3 - X_2)}{\sqrt{X_2^2 + Y_1^2} + \sqrt{X_3^2 + Y_1^2} - (X_3 - X_2)} \tag{6.4}$$

where Y_1, X_2 and X_3 are the partial coordinates of particular points in the WCS (see Section 9.4 for more details). They are calculated using (3.7), where the ICS coordinates $Y_{1,pix}$, $X_{2,pix}$ and $X_{3,pix}$ of those particular points appear, together with the camera and laser plane parameters U_c and $U_l = (e, \delta, \epsilon)$ (respectively) of the instrument. Using the same notation as in (6.1), we note $P_{pix} = (Y_{1,pix}, X_{2,pix}, X_{3,pix})$.

Let us suppose that the camera has been calibrated, inferring accurate values of the seven intrinsic parameters U_c defined in Section 2.4, and that N couples of images of a cylinder of known radius R_r have been acquired, at various distances between the instrument and the object.

For each couple of images $I_{on,i}$–$I_{off,i}$, it is possible to isolate, smooth and undistort the laser curve resulting from the projection of the laser plane on the object, by means of the image processing operations described in Chapter 5, and thus determine the coordinates $P_{pix,i}$ defined hereabove ($i = 1 \ldots N$).

The aim of the laser plane calibration is to iteratively determine the *best* value of U_l, i.e. minimizing the mean relative error on the radius, calculated on the N measurements. Before the first iteration, we have to:

- choose an initial set of laser plane parameters $U_{l,0} = (e_0, \delta_0, \epsilon_0)$, e.g. by means of raw measurements on the prototype;
- find an analytical expression of the partial derivatives of the relative error on the radius with regard to each laser plane parameter e, δ and ϵ. These are generally very long (and thus not reported here), but it is usually possible to decompose them in several smaller expressions easier to handle, using derivation tricks.

At iteration j ($j = 0 \ldots M$, where M is the maximum amount of iterations allowed by the user), for each measurement i, it is required to:

1. calculate the radius $R_{i,j}$ of the cylinder by (6.4), using $P_{pix,i}$ and $U_{l,j}$;
2. estimate the relative error $\rho_{R,i,j}$, using (6.2);
3. estimate the partial derivatives of the relative error with regard to the laser plane parameters $U_{l,j}$;
4. determine a *better* value for $U_{l,j+1}$, by taking the average of the N values of each parameter corrected by (6.3);

It is then possible to update the value of the mean relative error on the N measurements, and check whether the last iteration induced a non-negligible improvement ($> 10^{-3}\%$). If yes, the next iteration is processed. Otherwise, the procedure is stopped.

6.3.4 Performances

In order to evaluate the repeatability of the laser plane calibration procedure, we acquired 100 couples of images of four cylinders of known radii, at various distances between the instrument and the object, and performed 80 different calibrations, each time using 50 randomly chosen couples of images amongst the whole set. The dispersions on the parameter values are illustrated on Fig. 6.6. On sees that the standard deviation on the parameters is of the order of 0.1%, which is really excellent. See Section 7.4 to see the impact of this result on the accuracy of laser triangulation under structured lighting itself.

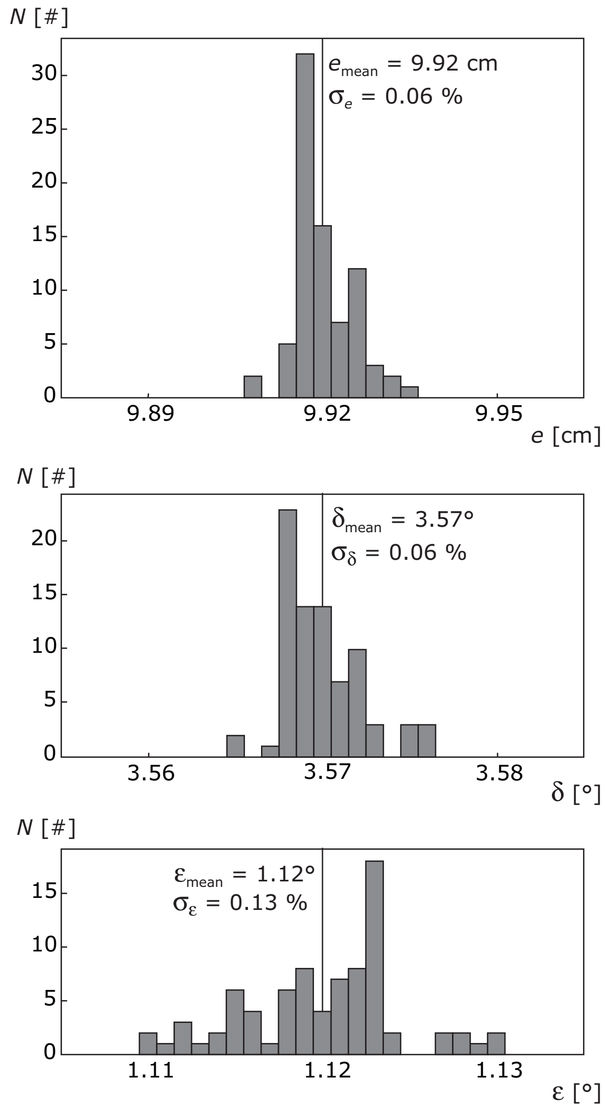

Fig. 6.6. Repeatability of the laser plane calibration, for e, δ and ϵ.